A Comparison of the Effect of Carbon Fiber and Silica Aerogel on Epoxy Composite Materials

Ze-Han Chen*, Ching-Lin Chen*, Ming-Horng Lin** and Tao-Hsing Chen**

Keywords: silica aerogel, carbon fiber, universal testing machine, Hopkinson bar

ABSTRACT

In this study, silica aerogel and short carbon fiber are added as reinforcements into NC826 epoxy resin to provide nano-macromolecular composite materials. The materials are subject to static compression and dynamic impact tests under various strain rates using a universal testing machine and Hopkinson bar. Field emission scanning electronic microscopy (FE SEM) is then used to obtain fractography to explore the mechanism of interfacial fracture and the dispersion of the reinforcements.

In the static test, the highest stress was obtained from the epoxy resin composite material with 0.4wt% short carbon fiber; in the dynamic test, it was obtained from the material with 0.6wt% carbon fiber. The SEM fractography shows that the addition of reinforcements in an appropriate amount is effective in improving the strength of epoxy resin, preventing the growth of existing cracks, and the transferring the stress along the substrate. Excess reinforcements can cause poor dispersion, leading to aggregation and loss of strength.

INTRODUCTION

Materials are closely related to the evolution of human civilization. Humans use a great variety of materials to achieve rapid technological improvement. With the expertise of material science, numerous materials have been developed to date. These can be categorized as metallic materials, ceramics materials, polymers materials (Liu et.al., 2022; Tan & Tan, 2017), semiconductors and composite materials (Chen et al., 2021; Shi et al., 2022; Thakur et al., 2014; Mohammed et al., 2024).

Macromolecular composite materials are widely researched and applied as a part of modern technology. In the general sense, such materials are the mixture of two or more materials of different natures to minimize or eliminate their innate disadvantages. More specifically, composite materials comprise substrate and reinforcements. The substrate transfers energy and combines with the reinforcements, with epoxy resin, phenolic resin, polyethylene resin and polyamide resin being more common. Reinforcements are available in various types, such as irregular, granular or fiber, with carbon fiber and glass fiber being more common, and boron fiber and Kevlar being less common (Avci et al., 2023; Peng et al, 2024; Singh & Samanta, 2015; Fu et al., 2018; Babazadeh et al., 2021). The conjunction of substrate and reinforcements is called the interface, which is the primary factor determining the binding strength of these materials and the superior performance when compared to each of the materials.

When combining the substrates and reinforcements in certain ratios, the resulting composite materials show better overall performance. The size of the reinforcements used is also a determining factor of performance, which has improved from micro-scale to nanoscale. These additives serve to prevent crack growth, material deterioration and stress concentration, and may even improve conductivity or corrosion resistance (Xu et al., 2022; Riaz et al., 2014; Hussain et al., 2019;

Paper Received February, 2025. Revised March, 2025. Accepted March, 2025. Author for Correspondence: Tao-Hsing Chen

** Graduate Student, Department of Mechanical Engineering, National Kaohsiung University of Science and Technology, Kaohsiung City, Taiwan 807618, ROC.*

*** Professor, Department of Mechanical Engineering, National Kaohsiung University of Science and Technology, Kaohsiung City, Taiwan 807618, ROC*

Radhamani et al, 2019). Consider that this expertise is still under vigorous development, it is warranted to further investigate into each of these materials. It is also expected that polymer materials, composite materials and nanomaterials will become an essential part of technological development.

EXPERIMENTAL METHOD

In this study, silica aerogel (Jang et al., 2021; Shi et al., 2020; Antony et al., 2023) and short carbon fiber are obtained with micro balance and transferred (at 0.2wt%, 0.4wt% or 0.6wt%) into glass volumetric glass filled with 10g butanone. The butanone mixture is subject to vortex mixing in a sonicator before pouring into the resin prepared with epoxy and curing agent at a ratio of 10:1 (100g epoxy and 10g curing agent is used based on calculation). A three-roll mill disperser is used to disperse the nanoparticles. The speed difference and gap between rollers create high shear that helps better dispersion of reinforcements in the material. While mixing, water cooler is used to keep the temperature of rolling pins at 13°C to manage the heat generated from friction which can lead to heat inflation, irregular gap width and leaching of impurities from these rolling pins.

After mixing, the resin is placed in a vacuum oven and heated to 70°C to minimize its viscosity and facilitate the elimination of the residual air. A plastic syringe is then used to extract the resin, which is slowly poured into a mold. The resin is then placed into a convection oven for curing. The cured resin is left to return to room temperature before the specimen is extracted and cut into the size needed for the test (7mm in diameter, 7mm in length) using low-speed diamond cutter.

The composite material specimen is used for mechanical property tests. The tests begin with static compression test using universal testing machine, in which the specimen is subject to compression at various speeds until structural failure to determine the relationship between stress-strain curve and strain rate. Dynamic impact test is performed using Hopkinson bar to determine the dynamic properties of the material. The fractured material is observed with scanning emission microscopy (SEM) to obtain fractography.

RESULT AND DISCISSION

Stress-strain curve

To determine the mechanical performance of epoxy composite materials added with each of the three reinforcements, the compression of the materials is further analyzed, with the process divided into two parts: Quasi-static and Dynamic.

Fig. 1 is the static stress-strain curve of pure epoxy resin, showing that stress increases with strain rate. In Fig. 2 to 4, it is shown that the stress also increases with aerogel content and strain rate. These three figures indicate that the addition of 0.2wt% silica aerogel provides the best performance. Fig. 5 to 7 also shows similar increase of stress with carbon fiber content and strain rate. These three figures indicate that the addition of 0.4wt% carbon fiber provides the best performance. A comparison of the static test result shows that the material added with 0.4wt% short carbon fiber has the highest stress.

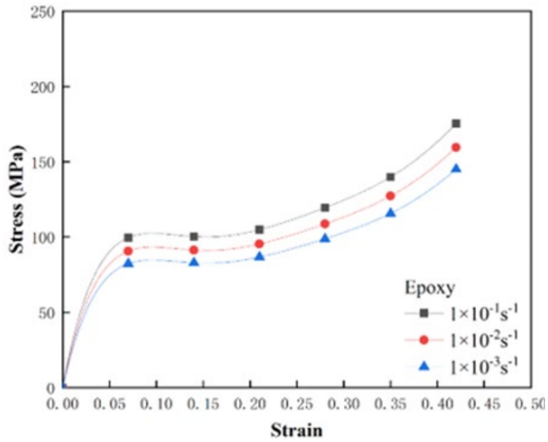

Fig. 1. The static stress-strain curve of pure epoxy resin.

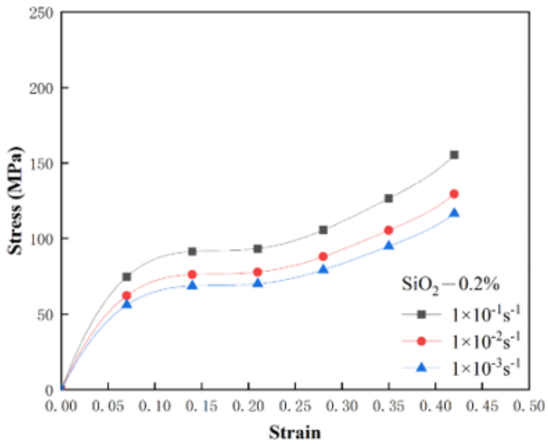

Fig. 2. The static stress-strain curve of resin added with 0.2wt% silica aerogel.

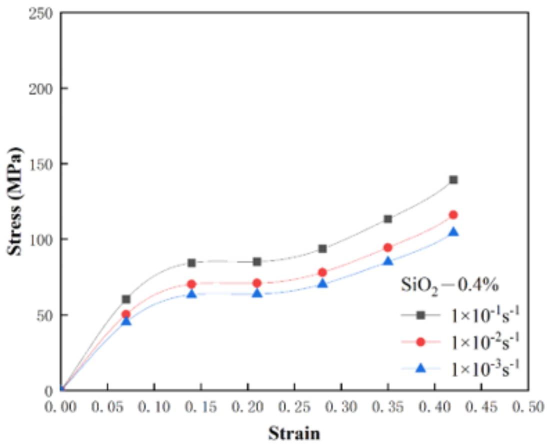

Fig. 3. The static stress-strain curve of resin added with 0.4wt% silica aerogel.

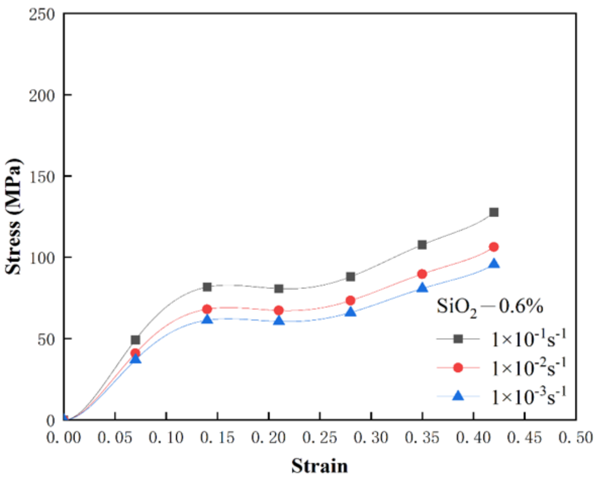

Fig. 4. The static stress-strain curve of resin added with 0.6wt% silica aerogel.

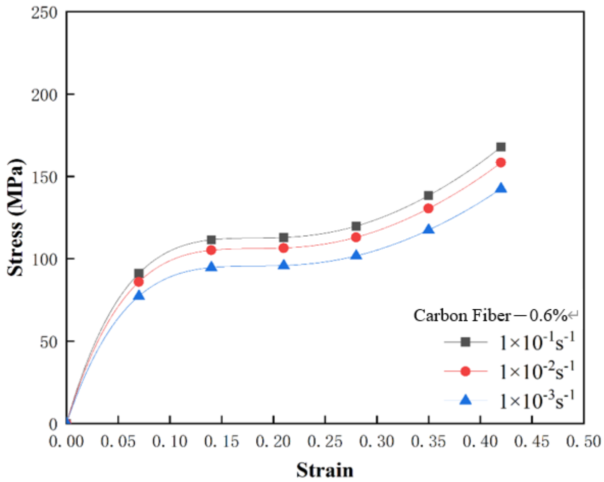

Fig. 7. The static stress-strain curve of resin added with 0.6wt% short carbon fiber.

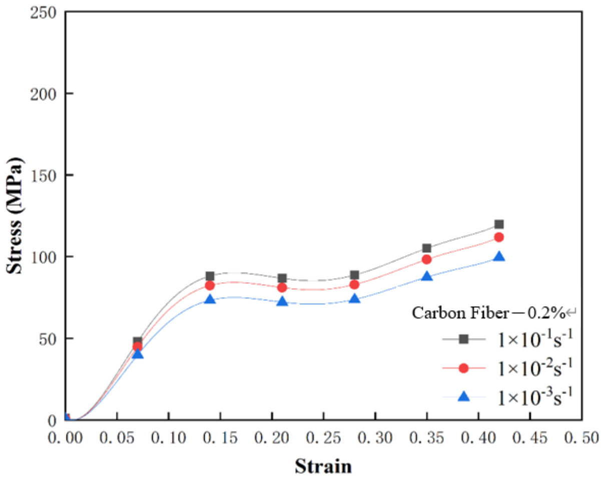

Fig. 5. The static stress-strain curve of resin added with 0.2wt% short carbon fiber.

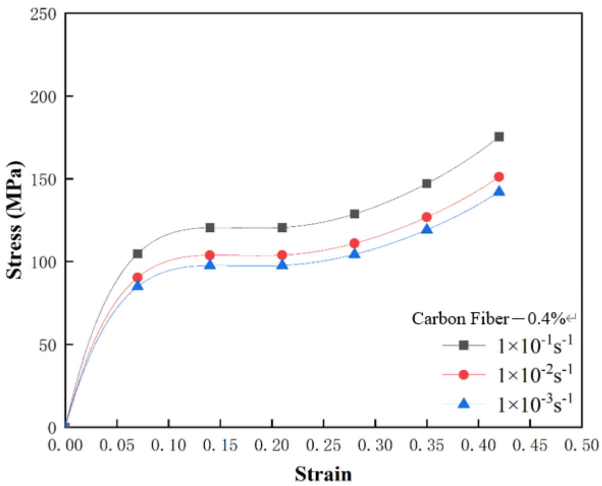

Fig. 6. The static stress-strain curve of resin added with 0.4wt% short carbon fiber.

Fig. 8 is the dynamic stress-strain curve of pure epoxy resin, showing that stress increases with strain rate. In Fig. 9 to 11, it is shown that the stress also increases with strain rate. These three figures indicate that the addition of 0.2wt% silica aerogel provides the best performance. Fig. 12 to 14 shows the dynamic stress-strain curve of epoxy composite resin added with carbon fiber in various ratios (0.2wt%, 0.4wt%, 0.6wt%). These dynamic stress-strain curves show that the stress increases with strain rate. These figures indicate that the material added with 0.6wt% carbon fiber showing the best performance. A comparison of dynamic test results shows that the material added with 0.6wt% short carbon fiber has the highest stress.

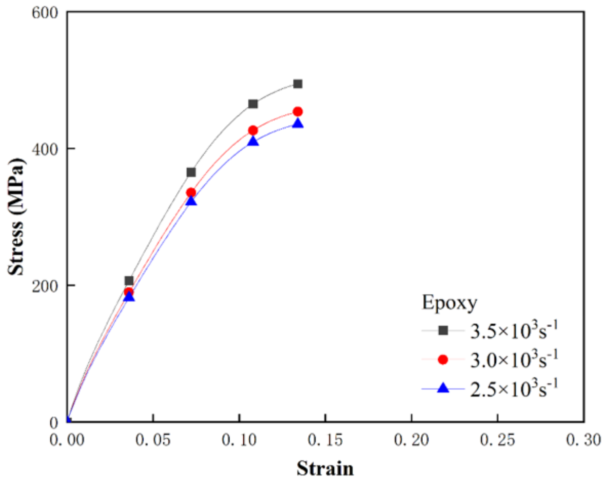

Fig. 8. The dynamic stress-strain curve of pure epoxy resin.

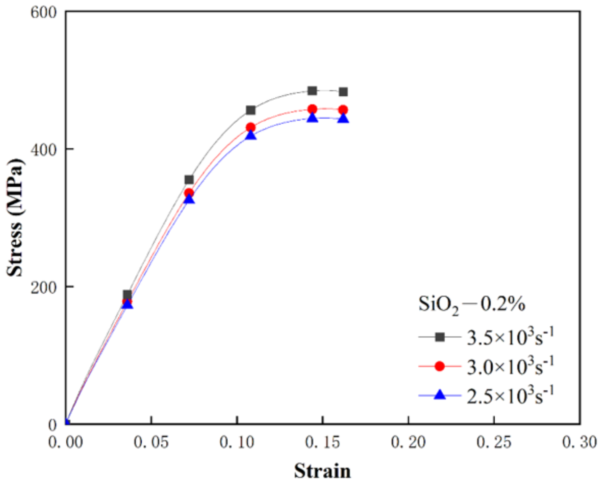

Fig. 9. The dynamic stress-strain curve of resin added with 0.2wt% silica aerogel.

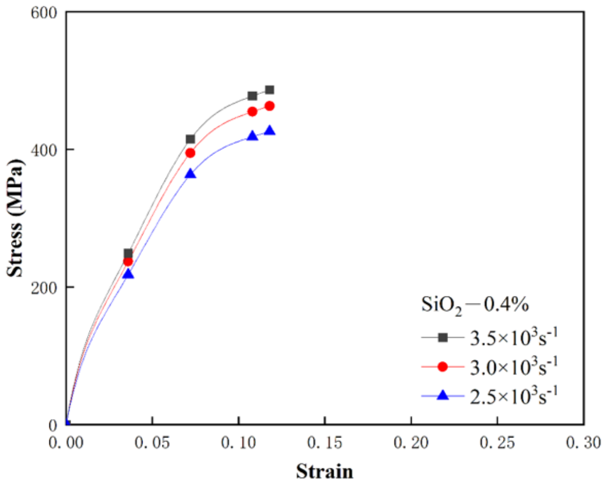

Fig. 10. The dynamic stress-strain curve of resin added with 0.4wt% silica aerogel.

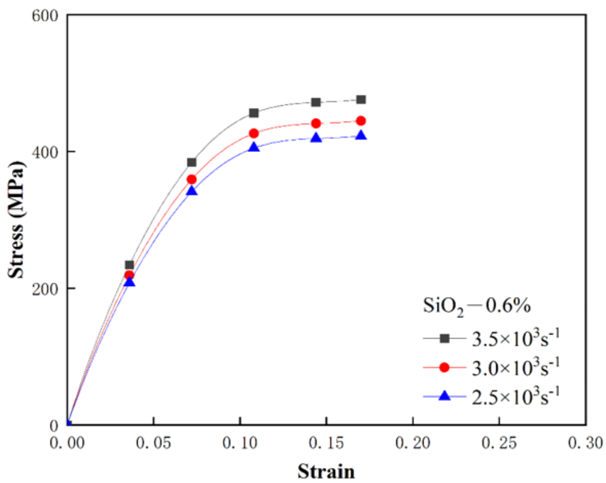

Fig. 11. The dynamic stress-strain curve of resin added with 0.6wt% silica aerogel.

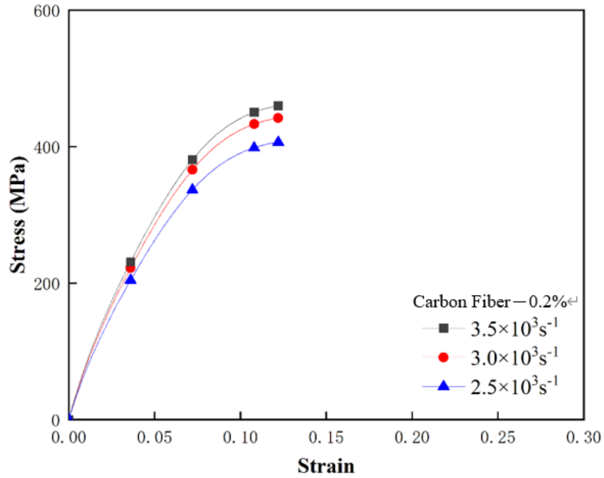

Fig. 12. The dynamic stress-strain curve of resin added with 0.2wt% short carbon fiber.

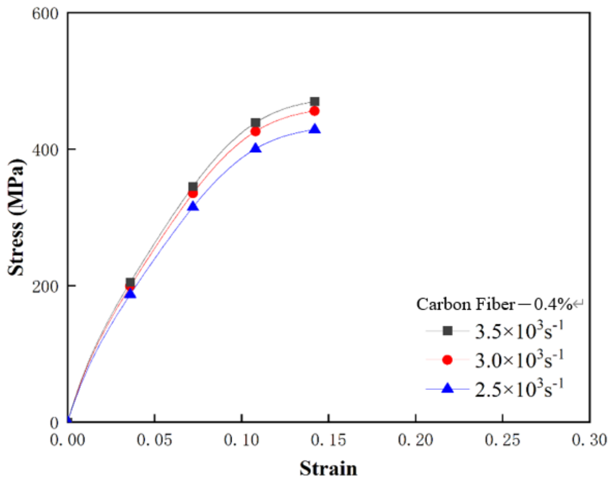

Fig. 13. The dynamic stress-strain curve of resin added with 0.4wt% short carbon fiber.

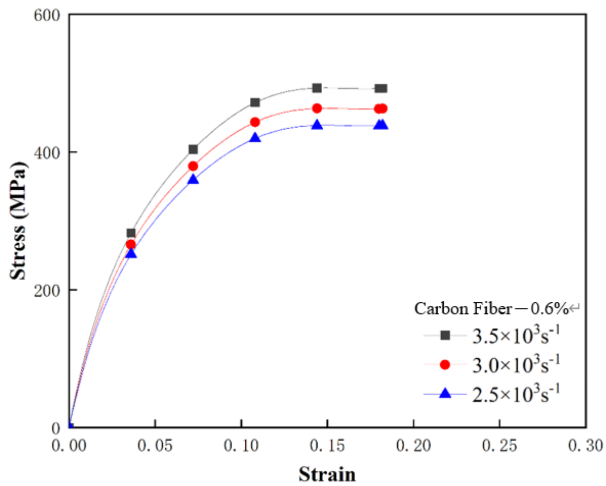

Fig. 14. The dynamic stress-strain curve of resin added with 0.6wt% short carbon fiber.

The relationship between yield strength and strain rate

To determine the mechanical performance of epoxy composite materials added with each of the three reinforcements, the compression of the materials is further analyzed, with the process divided into two parts: Quasi-static and Dynamic.

In static compression test, none of the specimens showed increase in yield strength, but a trend of reduction was observed. In the dynamic impact test, a slight reduction in yield strength was observed in the composite material added with 0.4wt% carbon fiber, and increase was observed in other specimens. The composite added with 0.2wt% silica aerogel showed the highest yield stress.

Fig. 15 to 17 present the relationship between yield strength and strain rate of materials added with 0.2wt%~0.6wt% silica aerogel or short carbon fiber. It is also found that the increase of yield strength is more apparent at higher strain rate, and the materials added with 0.2wt% silica aerogel have the highest yield stress.

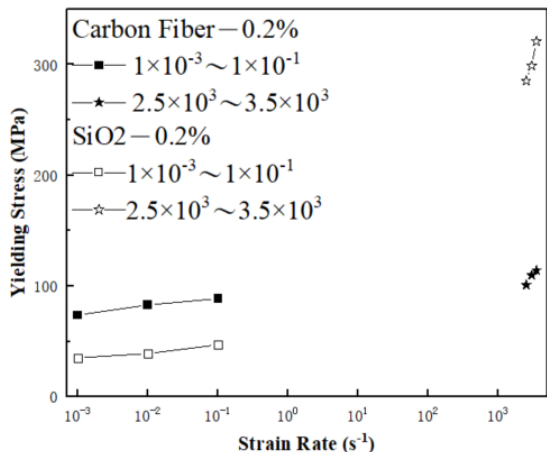

Fig. 15. The relationship of yield strength and strain rate observed in materials added with 0.2wt% silica aerogel and short carbon fiber.

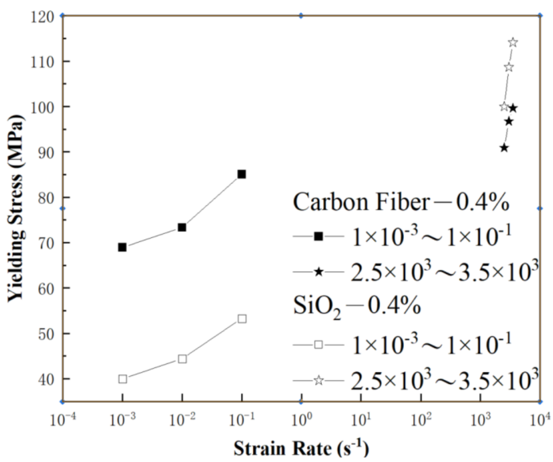

Fig. 16. The relationship of yield strength and strain rate observed in materials added with 0.4wt% silica aerogel and short carbon fiber.

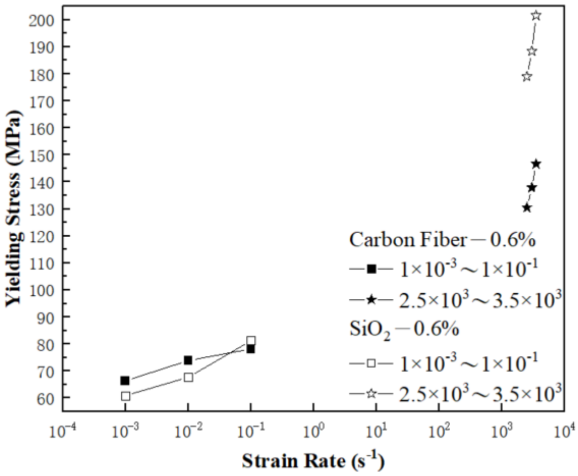

Fig. 17. The relationship of yield strength and strain rate observed in materials added with 0.6wt% silica aerogel and short carbon fiber.

By comparing the specimen of different content with the same strain rate, it is shown that the material added with 0.2wt% silica aerogel has the highest yield strength, indicating the proportional increase of yield strength with reinforcement content and strain rate.

The relationship between flow stress and strain rate

The stress-strain curve shows that strain rate significantly increases stress in composite materials added with reinforcements in different ratios. In this section, the relationship of flow stress and strain rate is discussed (Ma et al., 2021; Thiruppukuzhi & Sun, 2001; Lin et al., 2020).

Fig. 18 and 19 shows the relationship of static flow stress and strain rate under different strains (0.08 or 0.15). The figures show that the static flow stress increases (with strain) under the same strain rate, and under constant strain, the flow stress increases with strain rate.

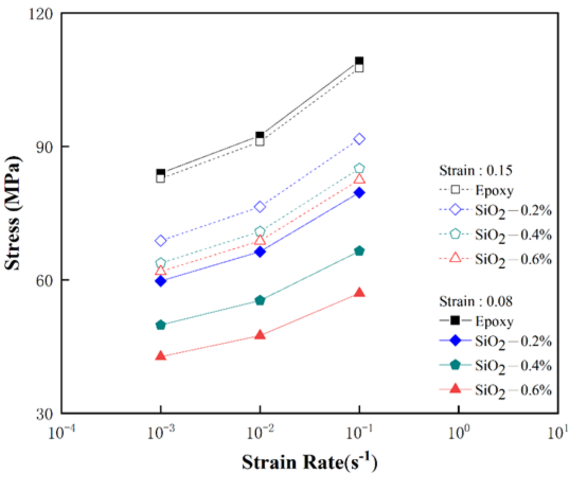

Fig. 18. The relationship between static flow stress of materials with aerogel and strain rate under various strain values.

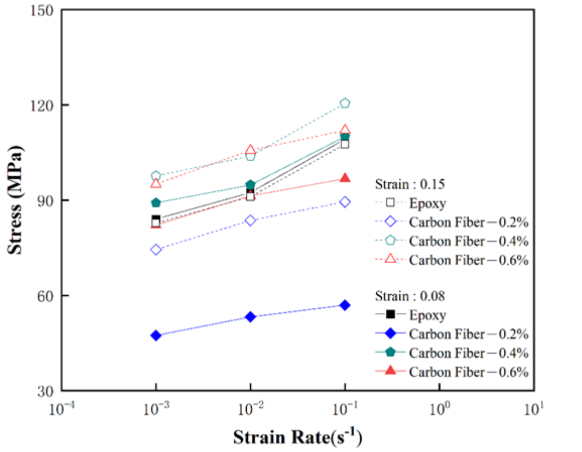

Fig. 19. The relationship between static flow stress of materials with carbon fiber and strain rate under various strain values.

Fig. 20 and 21 shows the relationship of dynamic flow stress and strain rate under different strains (0.08, 0.1) in materials added with aerogel and carbon fiber, respectively. The figures show similar trend.

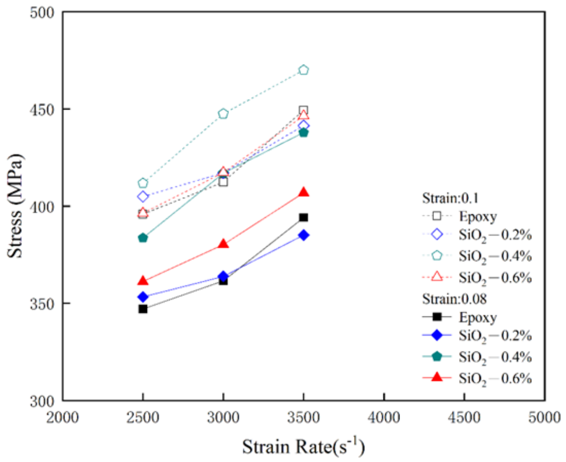

Fig. 20. The relationship between dynamic flow stress of materials with aerogel and strain rate under various strain values.

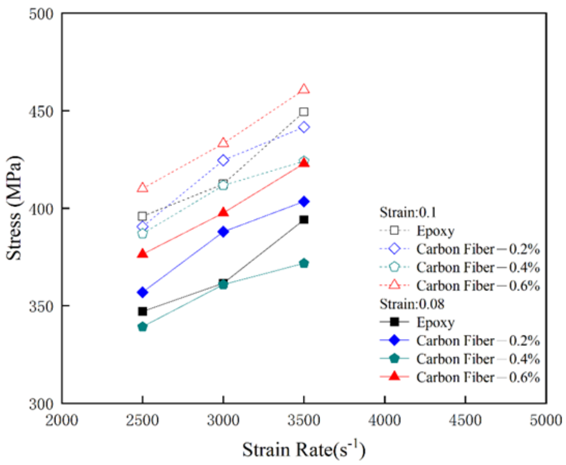

Fig. 21. The relationship between dynamic flow stress of materials with carbon fiber and strain rate under various strain values.

SEM fractography analysis

In this study, SEM is used to obtain microscopic fractography of nanomaterials. The SEM image in Fig. 22 shows that the epoxy resin without nanoscale reinforcements provide smoother fracture surface and crack growth, a typical finding of thermosetting polymers. This also suggests that the fracture propagation is less interrupted, making the resin prone to interface destruction as the cracks move and less toughness than the specimens with reinforcements (Jajam & Tippur, 2012; Singleton et al., 2003).

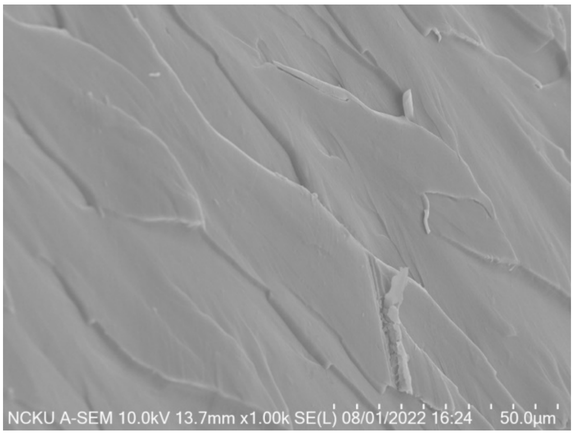

Fig. 22. Surface fractography of epoxy resin.

Fig. 23 to 25 clearly shows that silica aerogel on the fracture surface prevent crack growth or changes its direction of propagation. It can also be found that the silica aerogel is well dispersed and inhibits crack growth. Propagating small cracks would come to halt or change direction when reaching the reinforcements, which effectively prevent from crack growth and provide effective stress transfer along the substrate. Fig. 25 shows that the addition of 0.6wt% silica aerogel may cause poor dispersion and aggregation, and significant aggregation can reduce overall strength but increases toughness due to the gaps between nanoparticles, making the substrate more plastic and more effective in absorbing energy and reducing structural disruption.

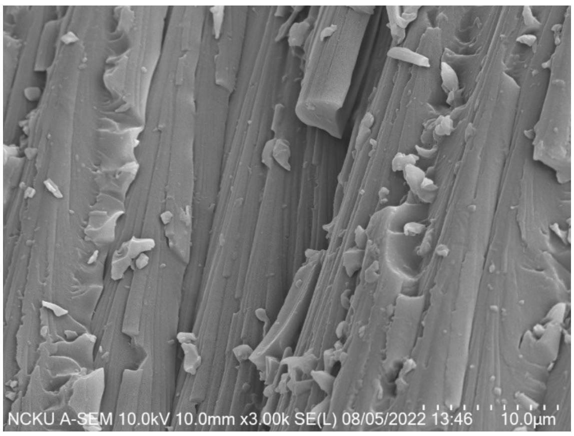

Fig. 23. The fractography of the material added with 0.2wt% aerogel (3000x SEM).

Fig. 24. The fractography of the material added with 0.4wt% aerogel (3000x SEM).

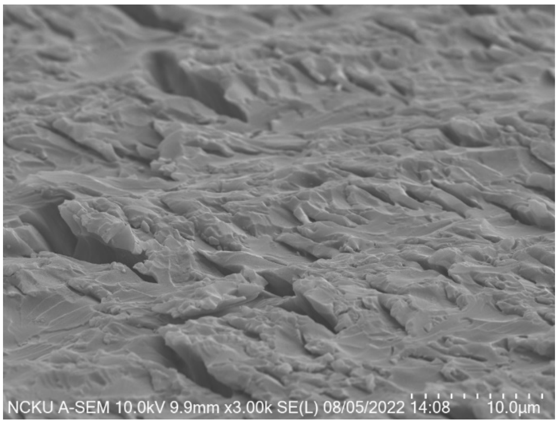

Fig. 25. The fractography of the material added with 0.6wt% aerogel (3000x SEM).

Fig. 26 to 28 clearly shows that carbon fiber on the fracture surface prevents crack growth or changes its direction of propagation. Fig. 26 shows that carbon fiber is well dispersed when added with 0.2wt% carbon fiber. Short fiber can be seen to be in the way of propagating cracks, inhibiting their growth. In Fig. 27 and 28, it can be seen that addition of 0.4wt% or more carbon fiber is associated with aggregation due to poor dispersion. It can be known that the well dispersion for the enhancement in the composite materials will have the well strength. The aggregation of enhancement will make the strength of composite decreased due to the the stress concentration.

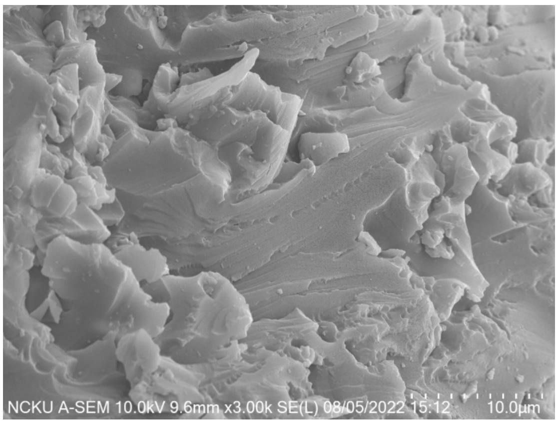

Fig. 26. The SEM fractography of the material added with 0.2wt% carbon fiber.

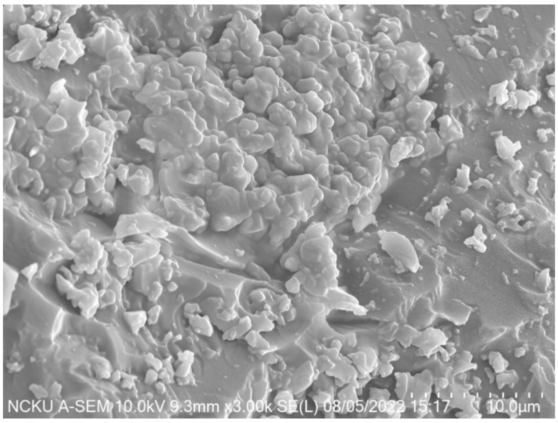

Fig. 27. The fractography of the material added with 0.4wt% carbon fiber.

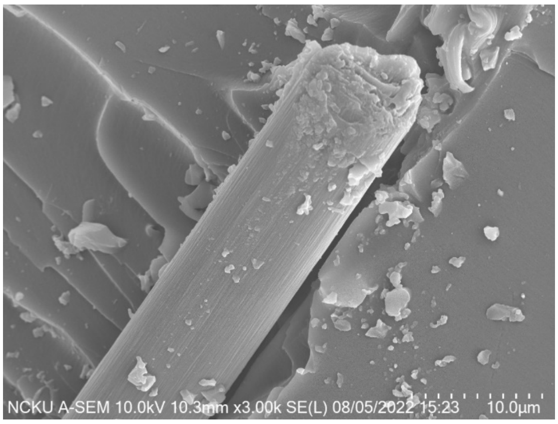

Fig. 28. The fractography of the material added with 0.6wt% carbon fiber.

CONCLUSION

1. In the static test, the highest stress was obtained from the epoxy resin composite material with 0.4wt% short carbon fiber; in the dynamic test, it was obtained from the material with 0.6wt% carbon fiber. When compared to pure epoxy resin, the addition of carbon fiber improves the composite material's mechanical properties.
2. At a constant strain of 0.08/0.15 and 0.08/0.1, flow stress increases with strain rate regardless of the strain rate.
3. The SEM fractography shows that the addition of reinforcements in appropriate amounts is effective in improving the strength of epoxy resin, preventing the growth of existing cracks, and the transferring the stress along the substrate. Excess reinforcements can cause poor dispersion, leading to aggregation and loss of strength.

ACKNOWLEDGEMENT

This article is the based on a study sponsored by the Ministry of Science and Technology (Program No.:

MOST 110-2628-E-992-002). We sincerely appreciate the support from MOST that facilitated the smooth completion of the study.

REFERENCES

Anthony, D. B., Nguyen, S. N., Qian, H., Xu, S., Shaw, C. M. D., Greenhalgh, E. S., Bismarck, A., & Shaffer, M. S. P. (2023). Silica aerogel infused hierarchical glass fiber polymer composites. *Composites Communications, 39*, 101531.

Avci, A., Eker, A. A., Bodur, M. S., & Candan, Z. (2023). Water absorption characterization of boron compounds-reinforced PLA/flax fiber sustainable composite. *International Journal of Biological Macromolecules, 233*, 123546.

Babazadeh, J., Rahmani, K., Hashemi, S. J., & Sadooghi, A. (2021). Effect of glass, carbon, and Kevlar fibers on mechanical properties for polymeric composite tubes produced by a unidirectional winding method. *Materials Research Express, 8*(4), 045301.

Chen, T. H., Wang, I. H., Lee, Y. R., & Hsieh, T. H. (2021). Mechanical property of polymer composites reinforced with nanomaterials. *Polymers and Polymer Composites, 29*(6), 696–704.

Fu, S., Yu, B., Tang, W., Fan, M., Chen, F., & Fu, Q. (2018). Mechanical properties of polypropylene composites reinforced by hydrolyzed and microfibrillated Kevlar fibers. *Composites Science and Technology, 163*, 141–150.

Hussain, A., Sudin, I., Basheer, U., & Yusop, M. (2019). A review on graphene-based polymer composite coatings for the corrosion protection of metals. *Corrosion Reviews, 37*(4), 343–363.

Jajam, K. C., & Tippur, H. V. (2012). Quasi-static and dynamic fracture behavior of particulate polymer composites: A study of nano- vs. micro-size filler and loading-rate effects. *Composites Part B: Engineering, 43*(8), 3467–3481.

Jang, D., Yoon, H. N., Seo, J., Park, S., Kil, T., & Lee, H. K. (2021). Improved electric heating characteristics of CNT-embedded polymeric composites with an addition of silica aerogel. *Composites Science and Technology, 212*, 108866.

Lin, C. F., Chen, T. H., Tsai, L., Hsieh, T. H., Su, W. C., & Wang, I. H. (2020). Investigation into quasi-static and dynamic tensile mechanical properties of aluminium–scandium alloy. *Materials Science and Technology, 36*(17), 1820–1828.

Liu, B. W., Zhao, H. B., & Wang, Y. Z. (2022). Advanced flame-retardant methods for polymeric materials. *Advanced Materials, 34*(1), 2107905.

Ma, L., Liu, F., Liu, D., & Liu, Y. (2021). Review of strain rate effects of fiber-reinforced polymer composites. *Polymers, 13*(17), 2839.

Mohammed, K., Zulkifli, R., Mat Tahir, M. F., & Gaaz, T. S. (2024). A study of mechanical properties and performance of bamboo fiber/polymer composites. *Results in Engineering, 23*, 102396.

Peng, F., Song, Y., Xu, T., Wang, M., Song, N., Sun, S., & Ding, P. (2024). Smart polymer composites with vertically oriented boron nitride and carbon fiber for heat management: Magneto-thermal responsiveness. *Composites Part B: Engineering, 283*, 111617.

Radhamani, A., Lau, H. C., & Ramakrishna, S. (2019). Nanocomposite coatings on steel for enhancing the corrosion resistance: A review. *Journal of Composite Materials, 54*(5), 681–701.

Riaz, U., Nwaoha, C., & Ashraf, S. M. (2014). Recent advances in corrosion protective composite coatings based on conducting polymers and natural resource derived polymers. *Progress in Organic Coatings, 77*(4), 743–756.

Shi, S. C., Chen, T. H., & Mandal, P. K. (2020). Enhancing the mechanical and tribological properties of cellulose nanocomposites with aluminum nanoadditives. *Polymers, 12*(1), 1246.

Shi, S. C., Lin, C. F., Liu, C. F., & Chen, T. H. (2022). Tribological and mechanical properties of cellulose/PMMA composite. *Polymers and Polymer Composites, 30*(1), 09673911221140935.

Singh, T. J., & Samanta, S. (2015). Characterization of Kevlar fiber and its composites: A review. *Materials Today: Proceedings, 2*(4–5), 1381–1387.

Singleton, A. C. N., Baillie, C. A., Beaumont, P. W. R., & Peijs, T. (2003). On the mechanical properties, deformation and fracture of a natural fibre/recycled polymer composite. *Composites Part B: Engineering, 34*(6), 519–526.

Tan, L., & Tan, B. (2017). Hypercrosslinked porous polymer materials: design, synthesis, and applications. *Chemical Society Reviews, 46*(10), 3322–3356.

Thakur, V. K., Thakur, M. K., & Gupta, R. K. (2014). Review: Raw natural fiber–based polymer composites. *International Journal of Polymer Analysis and Characterization, 19*(3), 256–271.

Thiruppukuzhi, S. V., & Sun, C. T. (2001). Models for the strain-rate-dependent behavior of polymer composites. *Composites Science and Technology, 61*(1), 1–12.

Xu, F., Zhang, M., Cui, Y., Bao, D., Peng, J., Gao, Y., Lin, D., Geng, H., Zhu, Y., & Wang, H. (2022). A novel polymer composite coating with high thermal conductivity and unique anti-corrosion performance. *Chemical Engineering Journal, 439*, 135660.